Real-Driving-Based Comparison of the Eco-Impact of Powertrain Concepts using a Data-Driven Optimization Environment

Eßer, Arved; Eichenlaub, Tobias; Rinderknecht, Stephan

(2020)

DOI (TUprints): https://doi.org/10.25534/tuprints-00011933

Publikationstyp: Conference or Workshop Item

Fachbereich: 16 Department of Mechanical Engineering

Quelle des Originals: https://tuprints.ulb.tu-darmstadt.de/11933

Real-Driving-Based Comparison of the Eco-Impact of Powertrain Concepts using a Data-Driven Optimization Environment

Arved Esser, **Tobias Eichenlaub**, **Stephan Rinderknecht**,
Technical University of Darmstadt

Abstract

In order to limit the effects of man-made climate change, the assessment of the ecological impact of different powertrain concepts is of increasing relevance and intensely studied. In this contribution we present a data-driven optimization environment that enables to identify the ecological potential of different concepts for different scenarios. The parametrization of each powertrain concept is dedicatedly optimized to minimize the ecological impact, which allows for an unbiased and reliable comparison on an uniform evaluation basis. To exploit the potential of each single powertrain parametrization, the operating strategy of the powertrain is adapted. Naturalistic driving profiles, including the speed, acceleration and road-slope information are depicted by multidimensional and representative driving cycles, allowing for an efficient search of the real-driving-optimal powertrain parametrizations within the optimization. In this study, we investigate long-range capable vehicles for a scenario in the reference year 2030 in Germany. Conventional vehicles, battery electric vehicles, fuel cell electric vehicles and plug-in hybrid electric vehicles are examined. Finally, the results are compared to an evaluation of the CO2 emissions according to the Worldwide harmonized Light vehicles Test Procedure (WLTP).

1 Introduction and Motivation

The increasingly visible effects of man-made climate change and its consequences [1] require to maximize the efforts of reducing the global greenhouse gas (GHG) emissions. Regarding the automotive sector, various studies have investigated the total GHG emissions of different powertrain concepts over the entire life cycle of the vehicle and this topic is prominently discussed in public debate. In most existent studies, typical representative vehicles are defined for each powertrain concept, based on available market vehicles. These representative vehicles are defined to depict typical parametrizations of the powertrain concepts regarding their components such as the electric machine and the battery.

The comparison of these representative vehicles is suited to compare state-of-the-art vehicles. However, these representative market vehicles are designed with various different objectives.

The vehicle's performance, the respective brand image or monetary costs are exemplary objectives that are considered in the development. Due to the differing development objectives, it remains unclear how the powertrain concepts would have performed in the comparison of GHG emissions if they had been specifically designed to minimize the ecological impact instead.

In [2], an optimization environment for the comparative analysis of the ecological potential of different powertrain concepts has been introduced for this purpose. For given scenarios and required design constraints of the vehicles, the powertrain parametrization is optimized towards minimal total GHG emissions over the life cycle of the vehicle (including production and End-of-Life), resulting in the ecological potential of a powertrain concept. By identifying this achievable minimum in the GHG emissions for each powertrain concept, a reliable and unbiased comparison of the different powertrain technologies is possible on a uniform evaluation basis.

The comparison of the GHG emissions of different powertrain concepts becomes increasingly complex due to various new developments such as the synthesis of fuels from electric energy (Power-to-X), that can potentially be supplied by renewable energy power plants. Furthermore, manufacturers are starting to take compensatory measures, such as planting trees, to argue that a certain vehicle is produced with an even GHG emissions balance. In future scenarios, all powertrain concepts could therefore potentially become nearly GHG-neutral if all the production and operation supply is based on renewable energies or if compensatory measures are taken. For this reason, it is meaningful to consider further quality measures, besides the GHG emissions, for the ecological assessment of powertrain concepts. Within this study, we additionally consider the total energy demand (TED). The TED quantifies the total electric energy, taken from the electric grid, to produce, operate and dispose a vehicle. For the operational phase, it is assumed that all fuels are synthesized via Power-to-X considering corresponding synthesis efficiencies. Especially for future scenarios that assume near 100 % renewable energies, the TED is suited to assess the eco-impact of different powertrain concepts.

Consensus in various different studies is that short-range battery electric vehicles (BEV) with a relatively small battery capacity perform very well in the comparison of the ecological impact of different powertrain concepts. On the other side, regarding long-range capable vehicles, different studies have been conducted. While [3] quantifies that BEV concepts outperform internal combustion engine vehicle (ICEV) concepts until very high ranges of 800 km for the reference year of 2019, [4] finds that fuel cell electric vehicles (FCEV) achieve smaller GHG emissions than BEV for ranges higher than 250 km. In [2], our team predicted that plug-in hybrid electric vehicles (PHEV) can lead to the lowest GHG emissions in 2030 for an exemplary range of 350 km, if the vehicles are optimally used and regularly charged electrically. From the presented studies, no general consensus about the most suitable powertrain concepts for long-range capable vehicles can be concluded. Therefore, we further investigate long-range capable vehicles in this work.

An additional limitation in available studies on the ecological impact of different powertrain concepts is the absence of studies that investigate all currently relevant powertrain concepts on a uniform evaluation basis, which might be part of the reason for the lack of consensus about long-range capable vehicles. PHEV or ICEV, driven by the combustion of compressed natural gas (CNG), and FCEV are often excluded from available studies. Furthermore, FCEV are mostly considered without external charging (plug-in) functionality. Within the present work, we incorporate all previously mentioned concepts into the optimization framework to provide a comprehensive comparison of the ecological potential of the presented concepts on a uniform evaluation basis.

Additionally, a significant impact factor on the resulting GHG emissions and TED are the considered driving profiles, that are used for the evaluation. As pointed out in various studies, the consideration of real-driving profiles resulting from the naturalistic driving of the relevant application is essential. To address this point, we perform our analysis for two given naturalistic driving profiles measured on public roads in the area of Darmstadt in Germany, that are characterized by the occurrence frequency of operating states concerning speed, longitudinal acceleration and road-slope. Further, the results of these real-driving profiles are compared to the method of the "Worldwide harmonized Light vehicles Test Procedure" (WLTP) for the quantification of GHG emissions.

In Section 2 of this work, the optimization framework for the comparative analysis of the eco-impact is presented. Section 3 provides details about the naturalistic driving data sets and the derivation of driving cycles applied in this study. Thereafter, the vehicle simulation model for the simulative evaluation of fuel (including hydrogen (H2) and CNG) and electricity demands is introduced. The results of the ecological potential concerning the GHG emissions and the TED are presented in Section 5 for the different driving profiles. Finally, we summarize the presented work and draw conclusions in Section 6.

2 Optimization Framework to enable an unbiased Comparison

As stated above, the assessment criteria for the vehicles to be compared in this work are the TED and the GHG emissions. Both measures are affected by various different factors in different phases of the vehicle life cycle. The GHG emissions are considered for the complete

life cycle including emissions during the operational phase, production and End-of-Life ('Cradle-to-Grave').
Concerning the TED, the energy chain from the grid to the demand for driving, i.e. 'Grid-to-Wheel' energy demand, is considered. This also incorporates the energy demand for the production of synthesized fuels. For the TED, it is assumed, that all fuels are synthesized via Power-to-X. Due to the current lack of detailed data for the energy demands in the production and End-of-Life phases for most powertrain components, only the production of the battery, as a main contributing component, based on [5], is considered.
The energy demand during the operational phase is further dependent on the powertrain type and the parametrization of the powertrain components like the energy converters, but also on the specific usage of the vehicle. A specific parametrization of a powertrain might be advantageous for a specific usage of the vehicle. For example, a higher peak power of the electric motor affects the vehicle’s consumption due to a higher vehicle weight and because it may be operated in less efficient operating points of the motor. This in turn requires a larger battery capacity to meet a specific range, which again leads to higher emissions during production of the battery. Therefore, an unbiased comparison of different powertrain concepts can only be ensured when the parametrization is optimized for the specific usage and for the respective assessment criterion.
To ensure an uniform evaluation basis for the different powertrain concepts, the consumption of the vehicles is determined on the same driving profiles and with the same minimal range requirements. To analyze the influence of the driving profile on the results, two different naturalistic driving profiles are examined in this work. Representative driving cycles are derived from the naturalistic driving profiles by a cycle synthesis method based on [6] that can be used to efficiently determine realistic consumptions of the vehicles. A detailed description of the naturalistic driving profiles and the derivation of representative driving cycles is given in Section 3. In addition to meeting the traction demand imposed by the driving cycle, technology neutral design constraints are defined for all powertrain concepts to ensure the general drivability of the vehicles. All vehicles must be able to meet multiple acceleration characteristics (0-60 km/h in 4,2 s, 0-100 km/h in 8,6 s, 80-120 km/h in 6 s). Additionally, a maximum speed of 180 km/h and a launch acceleration of 2,5 m/s² on a slope of 30 % are demanded.
As mentioned above, the optimization of the powertrain sizing and parametrization has the objective to minimize either the GHG emissions or the TED in order to create an unbiased basis for the comparison of the powertrain concepts’ potentials. For this purpose, a set of main design parameters d is defined that enable the encoding of a specific powertrain parametriza-

tion, shown in Table 1. Amongst others, they comprise of the peak powers of the energy converters (Internal Combustion Engine (ICE), Electric Machine (EM) and Fuel Cell (FC)) and the capacity of the battery C_{Batt}. More detailed information about the powertrain modelling based on these parameters is given in Section 4.

Table 1: Summary of the design parameters d that are optimized for every powertrain concept and for every driving profile both towards minimal GHG emissions and minimal Total Energy Demand.

N_{ICE}	Index of the internal combustion engine in the database
$P_{EM,max}$	Peak power of the electric machine
$P_{FC,max}$	Peak power of the fuel cell
C_{Batt}	Capacity of the battery
n_{Transm}	Number of speeds in the transmission system
i_n	Gear ratio of the transmission speeds i_1 to i_N
$i_{EM,Hybrid}$	Relative ratio of the connection of the electric machine for Parallel-Hybrid-Electric-Powertrains to the gearbox inlet

These design parameters are optimized with a genetic algorithm [7] using the presented assessment criteria as objective functions. The algorithm creates populations of encoded powertrain parametrizations, evaluates their respective fitness, i.e. the GHG emissions or TED, and iteratively creates new generations through selection, mutation and recombination methods. In every evaluation of the fitness function, an efficiency-oriented operating strategy of the vehicle is applied for each parametrization that is based on a locally optimal control approach. The operating strategy is adapted for every individual parametrization of the population to ensure the comparability of different parametrizations in the framework. Since the optimal encodings of the powertrains might differ for both objective functions as well as the considered driving profiles, all powertrain concepts are optimized separately for both objective functions and both driving profiles. The whole optimization framework described here is illustrated in Fig. 1.

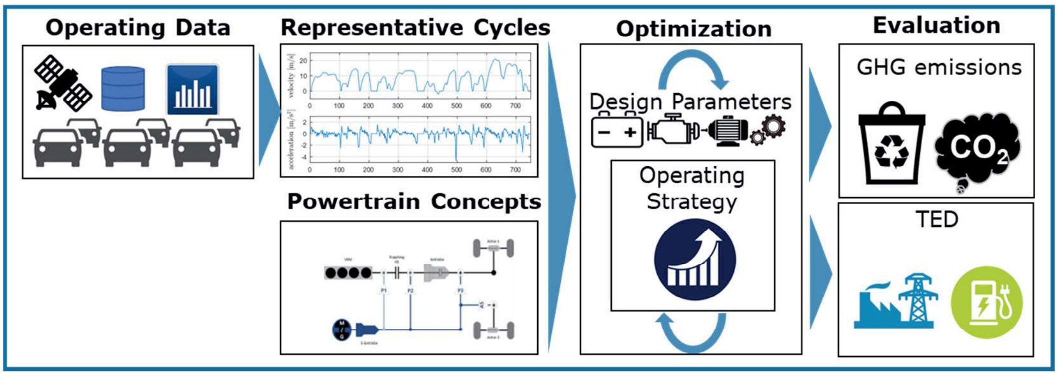

Fig. 1: Data-driven optimization framework for the comparison of the eco-impact of different powertrain concepts.

3 Naturalistic Driving Profiles

It has been shown that driving profiles differ significantly [8] and strongly influence a vehicles consumption [9]. Therefore, the considered driving profiles are of fundamental relevance in the simulative assessment of the eco-impact.

To enable an unbiased estimation of the ecological impact of the powertrain concepts, the real driving data from the relevant application must be considered. Since the chosen driving profiles have a significant impact on the resulting consumptions and powertrain parametrizations, we investigate two different naturalistic driving profiles, which allows us to analyze the differences with respect to the driving characteristics. The two driving profiles result from the naturalistic use of two vehicles that have been equipped with vehicle data loggers. The first driving profile comprises of tracks recorded with a pool-vehicle at TU Darmstadt (pool-vehicle profile), which is operated by various different drivers for business purposes. The second driving profile was recorded with the private vehicle of a single employee of TU Darmstadt (employee profile) which is only driven by this person. However, the here presented method could be repeated with any given driving profile, from a certain application field (certain drivers, regions, vehicles classes etc.) enabling to quantify the potential of different powertrain concepts for the specific driving profile.

For the two real-driving profiles, the vehicle's speed and longitudinal acceleration as well as the GPS positions are recorded for this study. From the GPS position, the elevation is interpolated with the free topology data from the "Radio Shuttle Topology Mission" (RSTM) [10]. The road-slope is estimated based on the elevation and speed information. In summary, the driving profiles can be regarded as three-dimensional matrices that contain the occurrence frequency of operating states in the speed, acceleration and road-slope dimension. In Fig. 2, two-dimensional representations of the three-dimensional pool-vehicle profile are shown by adding all occurrence frequencies in the respective missing third dimension. The pool-vehicle profile is characterized by rather dynamic driving with high top speeds and accelerations at higher speeds. Furthermore, the different drivers frequently use adaptive cruise control (ACC) with commonly selected desired speeds resulting in various visible peaks in the pool-vehicle profile on the zero acceleration axis.

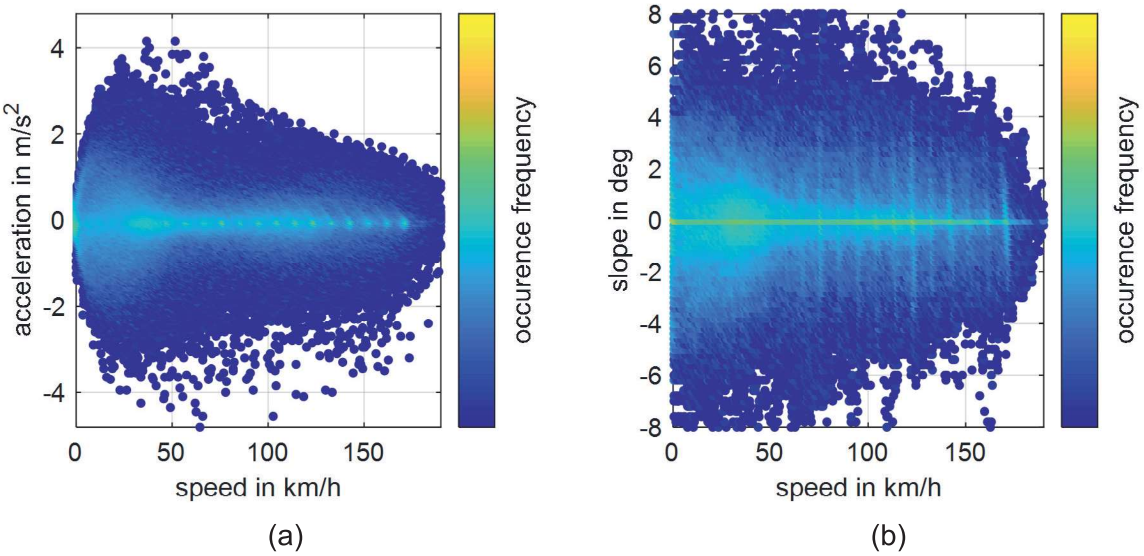

Fig. 2: Illustration of the pool-vehicle profile. 9077 km of operating data have been recorded. SubFig. (a) shows the occurrence frequency of operating states in the speed-acceleration plane from the three-dimensional driving profile. SubFig. (b) shows the occurrence frequency in the speed-slope plane.

In the following, we present, how the driving profile is considered in the optimization framework in detail for the pool-vehicle profile. The same approach is applied for the employee profile.

Within the previously presented optimization framework, representative driving cycles are used to depict the entirety of the driving profiles data in a compressed manner. As mentioned before, the use of the representative driving cycles allows to evaluate the characteristics of a high number of powertrain parametrizations very efficiently within the optimization, compared to the consideration of all the data for each powertrain parametrization. We apply the driving cycle synthesis method presented in [6] to generate multidimensional and representative driving cycles, including the road-slope in addition to the vehicle speed and acceleration. The synthesis procedure is able to maintain the physical dependencies between the speed, acceleration and road-slope signal from the original data within the generated cycles [6].

For vehicle powertrain concepts with only one energy source, like ICEV and BEV, we could compress the entire driving data of a driving profile into a single cycle since the consumption only depends on the occurring operating states. However, in the case of plug-in hybrid concepts with two energy sources, such as PHEV and fuel cell plug-in hybrid electric vehicles (FCPHEV), the consumption also depends on the distance of the tracks. Shorter tracks allow for an increased percentage of electric driving compared to longer tracks. The PHEV might drive a short track completely electrically, but needs to use the combustion engine for longer tracks (even if the tracks have equal operating points) to achieve the desired range. Therefore, the distribution of trip distances, shown in Fig. 3 for the pool-vehicle profile, has to be considered for each driving profile. On the left, the number of trips for different distances are illustrated showing that most trips are rather short. On the right, the cumulative proportion of driven kilometers from the total mileage of the driving profile is shown. A significant share of nearly 50 % of the driven kilometers is performed on tracks with a distance between 120 and 170 km despite the relatively small number of these trips.

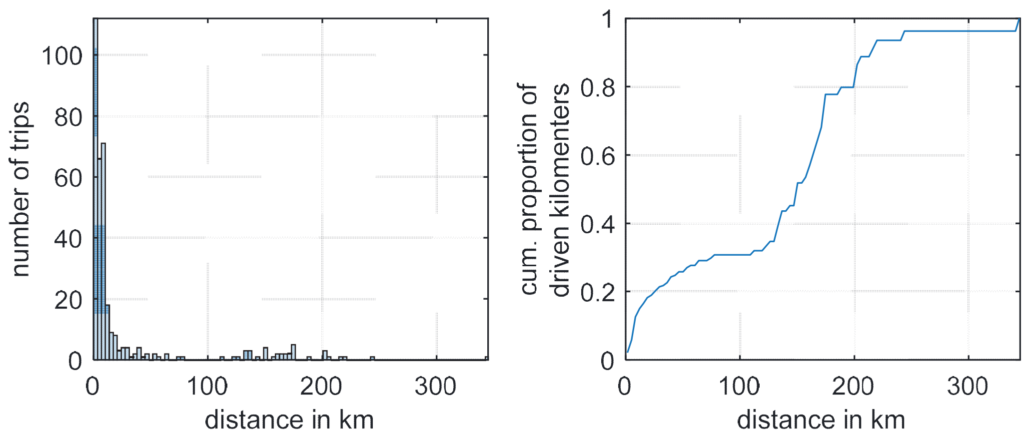

Fig. 3: Distribution of trips and driven kilometers over the trip distance. A total of 9077 km has been recorded for the pool-vehicle profile.

To consider the distance distribution within our model, we assign the available driving data to multiple distance clusters, using the 'k-means' algorithm. Each distance cluster contains all tracks from a certain distance range. Each cluster represents a driving subprofile for which a representative driving cycle is synthesized. The driving cycles are then used in the vehicle simulation model of the optimization framework with distances of the corresponding cluster centers.

The number of distance clusters is a trade-off between a low variance of distances inside a cluster, to avoid that tracks are assigned to cluster centers far from their original distance, and a sufficiently large number of tracks inside a cluster to enable a meaningful compression of the data through the cycle synthesis. Further, each distance cluster requires a driving cycle simulation for each parametrization of a powertrain concept within the optimization leading to increased computational effort. To identify an adequate number of distance clusters, we repeat the k-means clustering with multiple cluster numbers and analyze the distribution of the distance deviation of the tracks from their assigned cluster centers using boxplots as shown in Fig. 4. The boxplots show the maximum deviation, the 2-sigma interval, the 25 % and 75 % quantiles as well as the median deviation. Until a number of 5 clusters, the maximum distance difference of the tracks decreases significantly. The 2-sigma interval, the 75 % quantile and the median distance stay nearly constant from two to four clusters, but there is a significant improvement for five clusters. From five to eight clusters, these values stagnate again. Therefore, we use a cluster number of five for the pool-vehicle profile as a good compromise of computational effort and modelling accuracy.

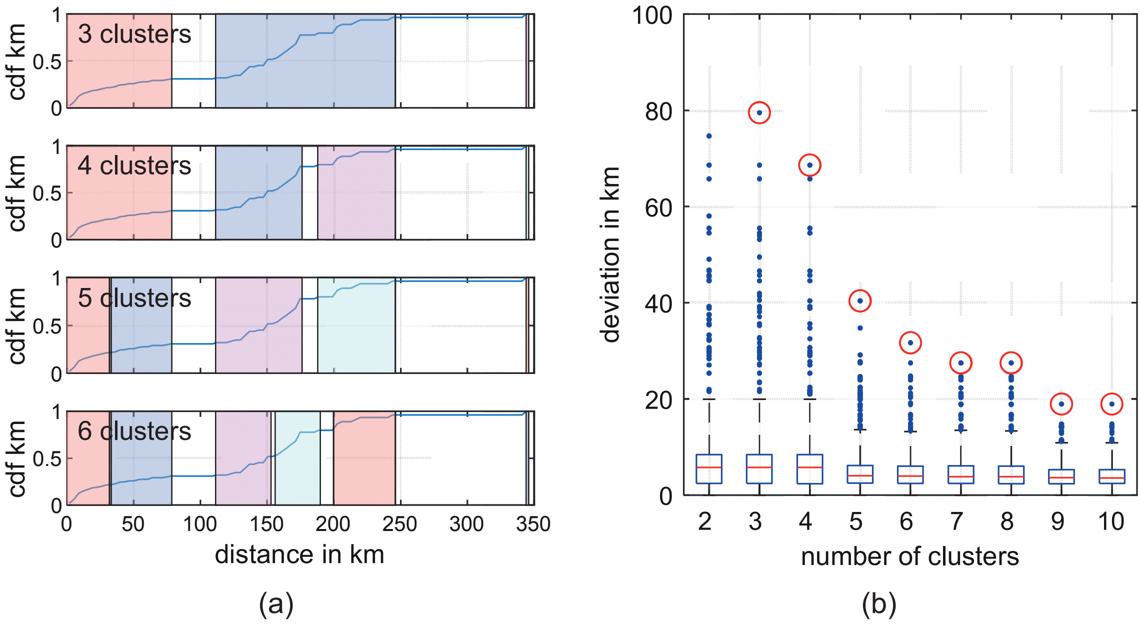

Fig. 4: Results from the cluster analysis of tracks in the pool-vehicle profile. SubFig. (a) shows the results of the clustering for three to six clusters with the cumulative density function (cdf) of the driven kilometers. SubFig. (b) shows the boxplots of the deviations of all track distances to their assigned cluster centers in kilometers. The maximum deviation is marked with a red circle. Tracks with a deviation above the 2-sigma interval are marked with blue dots. The 2-sigma interval is shown with a black line. The 25 % and 75 % quantile are shown with blue boxes. The median is indicated by the red line.

For each of the five chosen distance clusters, we synthesize 10,000 representative driving cycles using the method presented in [6]. From the multitude of cycles of every cluster, we chose the cycle with the lowest error in the speed-acceleration-slope frequency distribution (SASFD) e_{SASFD}.

$$e_{\mathrm{SASFD}} = \frac{1}{2} * \sum_{n} \left| \frac{t_{\mathrm{ref},n}}{t_{\mathrm{ref,tot}}} - \frac{t_{\mathrm{syn},n}}{t_{\mathrm{syn,tot}}} \right| \quad (1)$$

The e_{SASFD} sums up the relative difference of times t spent in state *n* between the cluster profiles and the synthesized cycles. The states *n* consist of the combinations of speed, acceleration and road-slope that occurred in the driving profile. Additionally, cycles with a difference in elevation from start to end are omitted to maintain balanced recuperation potentials.

Fig. 5 shows the subprofiles of the five distance clusters in the speed-acceleration plane and the chosen cycles with minimal SASFD error that fulfil the elevation constraint. As expected, the driving cycles of the clusters for higher distances contain a larger amount of high-speed driving and less frequent acceleration or deceleration manoeuvres than the cycles of short distance clusters.

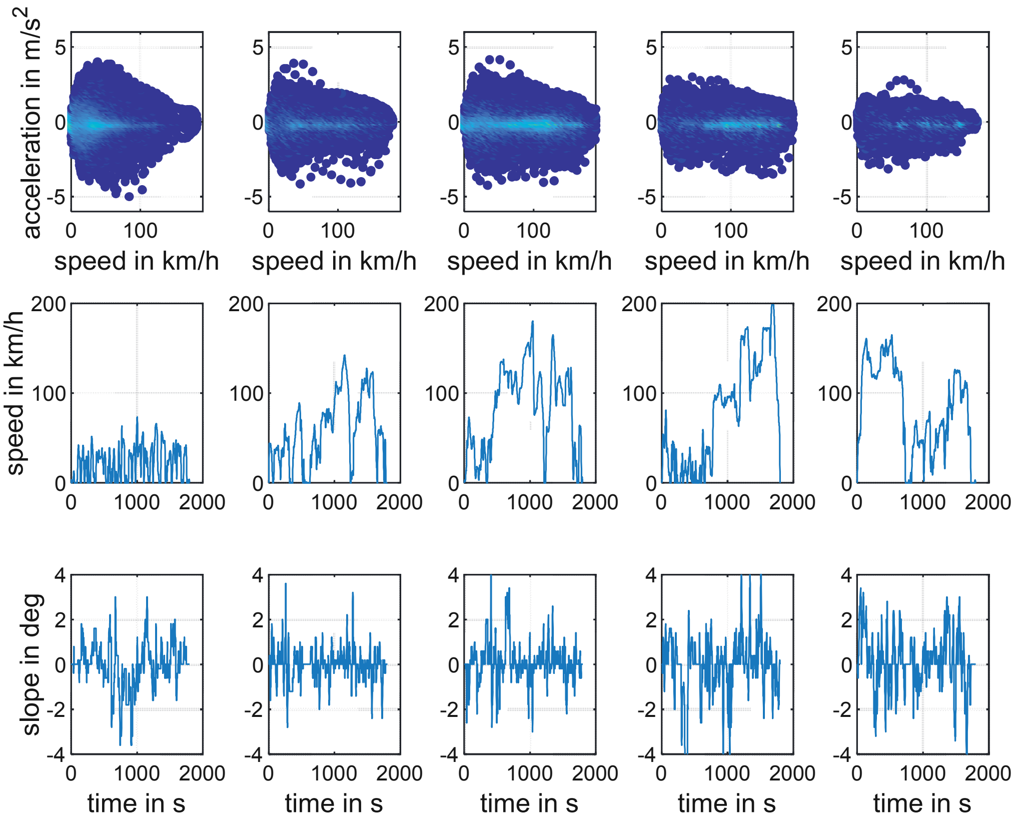

Cluster 1	Cluster 2	Cluster 3	Cluster 4	Cluster 5
Center = 12 km	Center = 53 km	Center = 155 km	Center = 211 km	Center = 345 km
Mileage weight	Mileage weight	Mileage weight	Mileage weight	Mileage weight
20 %	9 %	48 %	19 %	4 %

Fig. 5: Sub driving profiles from the five distance clusters of the pool-vehicle profile together with the synthesized driving cycles for each of the five clusters. Furthermore, the cluster center distances and the mileage-weights of the cycles are denoted.

For each cluster and corresponding driving cycle, the distance of the cluster center and the driven percentage of the total mileage within the cluster are summarized in Fig. 5. The mileage-percentage is used to weight the consumption values, identified by the vehicle simulation model on the different driving cycles to a total mean consumption.

The two-dimensional projections of the employee driving profile are shown in Fig. 6. The employee profile is characterized by more efficiency-oriented driving at moderate speeds and accelerations, compared to the pool-vehicle profile. During highway driving, the ACC system was applied frequently with a set speed of 120 km/h, visible in the profile 120 km/h and zero acceleration.

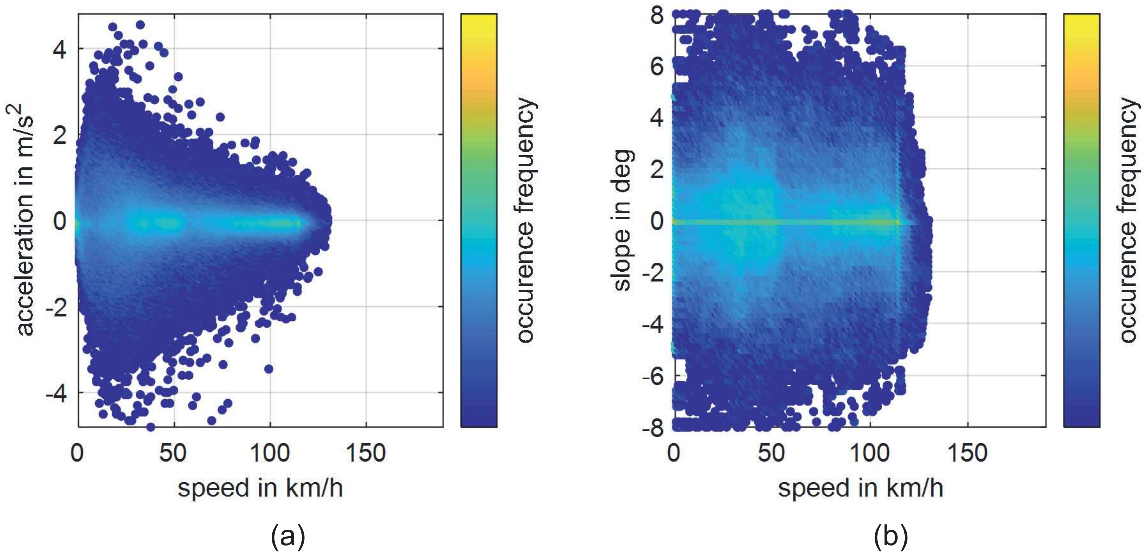

Fig. 6: Illustration of the employee profile. 8193 km of operating data have been recorded. SubFig. (a) shows the occurrence frequency of operating states in the speed-acceleration plane from the three-dimensional driving profile. SubFig. (b) shows the occurrence frequency in the speed-slope plane.

From the cluster analysis, we derive a number of four clusters for the employee profile, which results in similar key values (max deviation, 75 % quantile and median) in the distance deviation of the tracks from their assigned cluster centers compared to the pool-vehicle profile. The information about the clusters is summarized in Fig. 7.

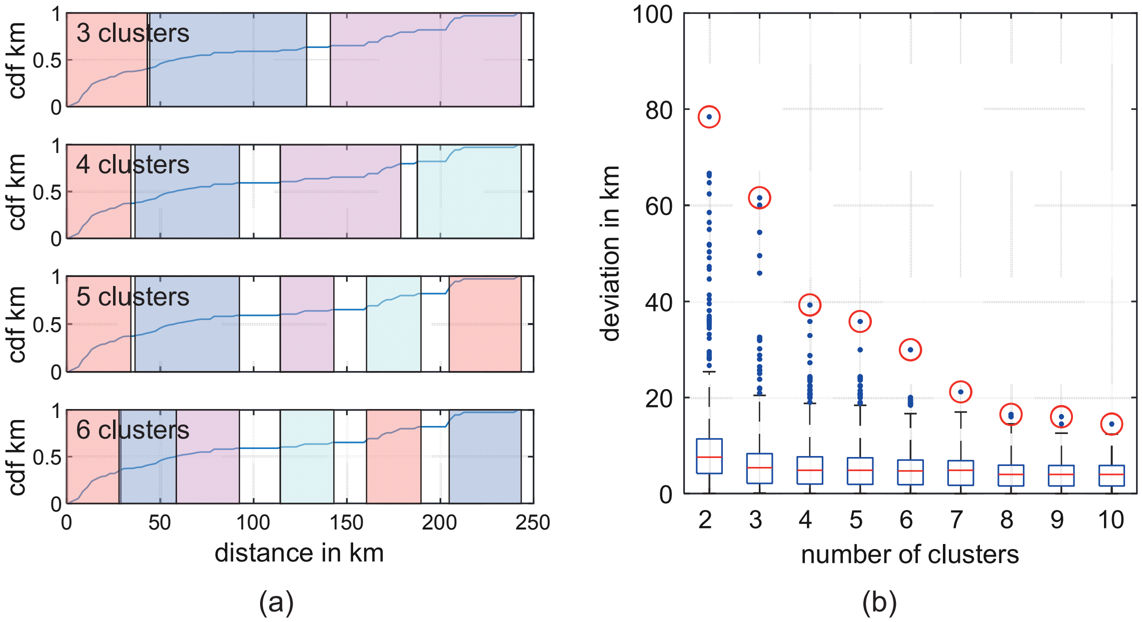

Fig. 7: Results from the cluster analysis of tracks in the employee profile. SubFig. (a) shows the results of the clustering for three to six clusters with the cumulative density function (cdf) of the driven kilometers. SubFig. (b) shows the boxplots of the deviations of all track distances to their assigned cluster centers in kilometers. The maximum deviation is marked with a red circle. Tracks with a deviation above the 2-sigma interval are marked with blue dots. The 2-sigma interval is shown with a black line. The 25% and 75% quantile are shown with blue boxes. The median value is shown with a red line.

As can be seen from the Fig., the longest track of the employee profile is around 250 km, compared to a maximum track length of 345 km in case of the pool-vehicle profile. In order to achieve a better comparison between the two naturalistic driving profiles, we use an equal minimum range requirement for both profiles. Therefore, we will simulate the driving cycle from the last distance cluster of both driving profiles twice. At first, with the respective center distance and mileage weight. Secondly, with a range requirement of 380 km, which corresponds to the longest track of the pool-vehicle profile and a 10 % 'buffer', and a mileage weight of zero. This represents an equal long-range requirement for both profiles, but will not directly affect the consumption values of the profiles, since the mileage weight is set to zero.

The best synthesized driving cycles for each distance cluster of the employee profile are shown in Fig. 8. The cycles for higher distance clusters are characterized by fewer stops and fewer acceleration and deceleration manoeuvres.

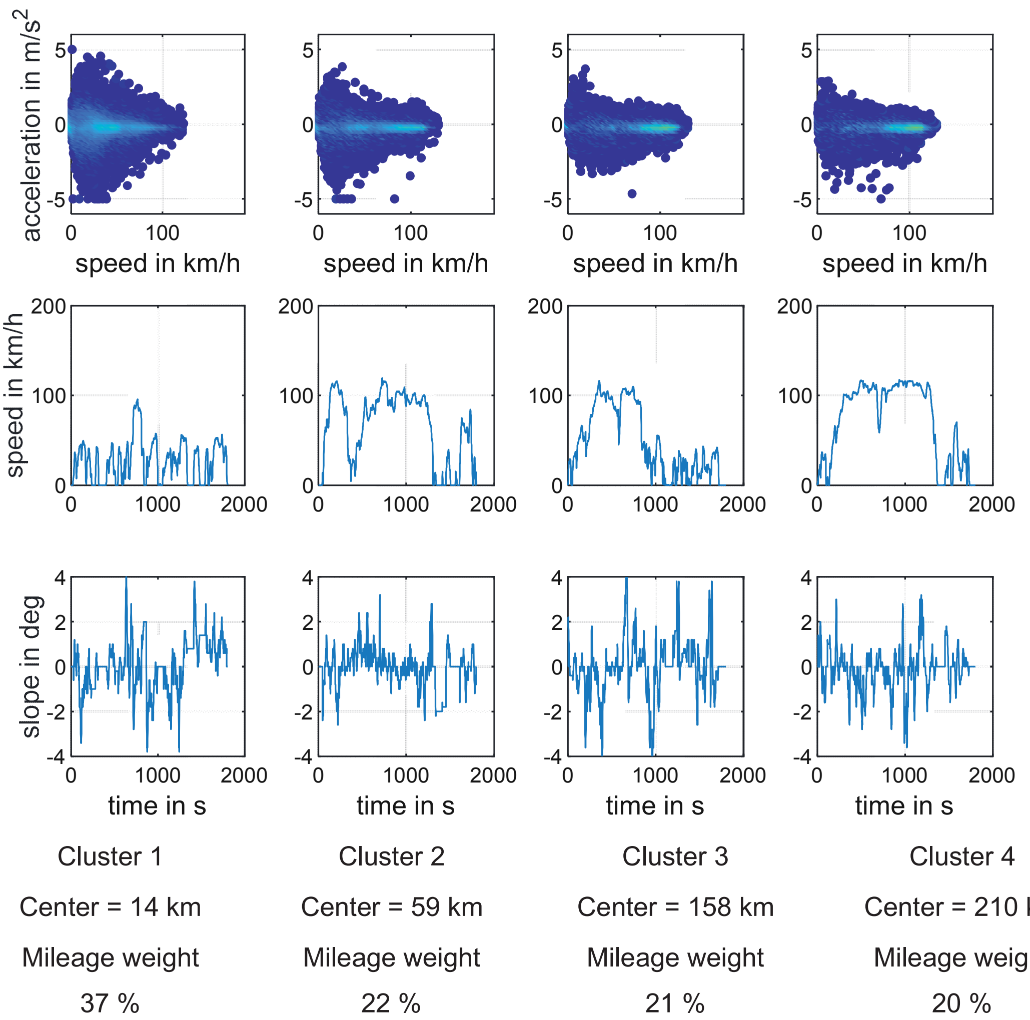

Fig. 8: Sub driving profiles from the four distance clusters of the employee profile together with the synthesized driving cycles for each of the clusters. Furthermore, the cluster center distances and the mileage weights of the cycles are denoted.

In this work, we also compare our approach to the evaluation of GHG emissions using the WLTP. The use of the presented optimization framework for the WLTP would not deliver plausible powertrain parametrizations due to the missing consideration of GHG emissions in the production, in the electricity and fuel supply and in the End-of-Life. Therefore, we consider the powertrain parametrizations from the optimization towards the GHG emissions for the pool-vehicle profile and compare the results of the WLTP and total GHG emissions evaluation. To depict the method of the WLTP, we simulate the Worldwide harmonized Light Duty Test Cycle (WLTC) two times using a charge-depleting and a charge-sustaining strategy. The fuel and electric consumptions of the two simulations are then weighted by the utility factor for the estimated electric range on the WLTC. The estimated GHG emissions of the WLTP evaluation result exclusively from the tailpipe emissions. The WLTC and the range dependent utility factor are shown in Fig. 9. Road-slopes and secondary demands, for example for the climatization of the cabin, are not considered for the WLTP evaluation.

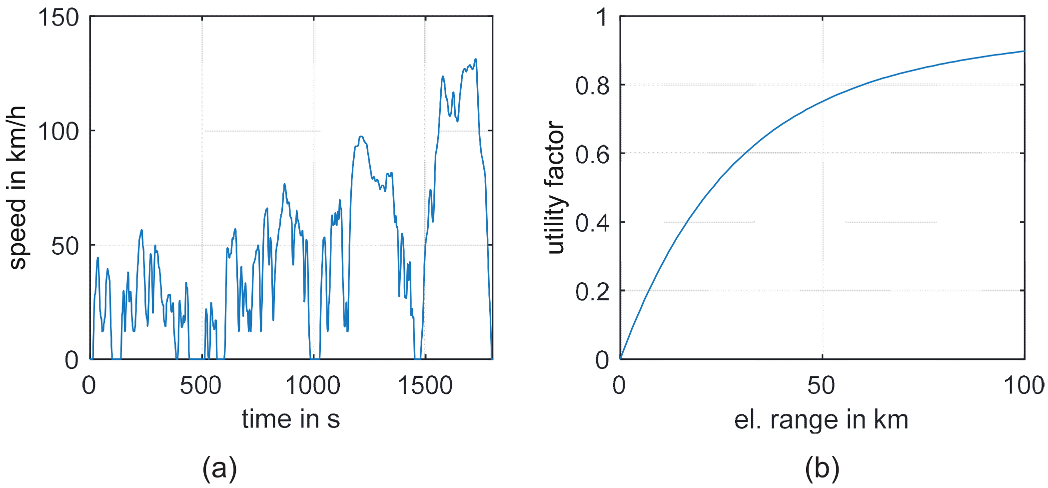

Fig. 9: SubFig. (a) shows the speed over time for the WLTC. In (b), the utility factor dependent of the electric range on the WLTC is illustrated.

4 Vehicle Simulation Model

To calculate the consumption of the powertrain concepts, a vehicle simulation model is integrated into the optimization framework. Inputs to the model are the design parameter set d, which is chosen by the optimizer and determines the parametrization of a single powertrain variant, and the driving cycles derived from the driving profile. The consumption of different powertrain concepts that is calculated in the vehicle model is then used to calculate the TED or to calculate the emissions in the operational phase as one part of the total GHG emissions of the vehicle. In addition to the primary consumption for moving the vehicle, a secondary energy demand is considered in the model that represents the energy demand of auxiliary systems like Heating, Ventilation and Air Conditioning. For a more detailed description of the secondary energy model, we refer to [11].

To differentiate between multiple powertrain concepts, a generic powertrain model is defined that consists of energy converters, a battery and three sub-transmissions TM1-TM3. The resulting tractive force is transmitted to one of the wheel axles. A specific powertrain concept can thus be built up by employing or omitting parts of the total powertrain model. The model and the connections of the different parts are shown in Fig. 10.

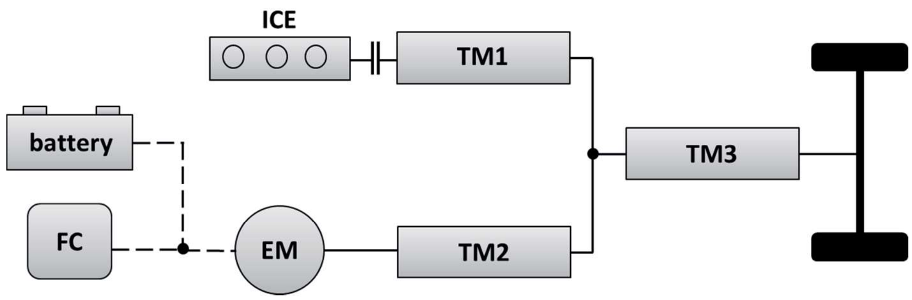

Fig. 10: Generic powertrain model used in this work. All of the analyzed powertrain concepts are derived from this model.

In this work, we examine conventional internal combustion engine vehicles (ICEV) with petrol and CNG engine, two battery electric vehicles, one with a fixed gear ratio (BEV-1) and one with a 2-speed transmission (BEV-2), fuel cell electric vehicles with and without plug-in functionality (FCPHEV and FCHEV) and plug-in hybrid electric vehicles (PHEV) with internal combustion engines (petrol E10 and CNG). The relevant parts of the generic powertrain model that are used for every powertrain concept are given by a binary encoding of the powertrain and is summarized in Table 2.

Table 2: Overview of the powertrain concepts analyzed in this work. The powertrain of a specific concept is built from the generic powertrain through the binary encoding (1 means existing, 0 means non-existing).

Class	Concept	Description	Binary encoding (ICE,EM,FC,TM1, TM2,TM3,battery)
ICEV	ICEV-E10	Conventional vehicle with petrol engine	(1,0,0,1,0,0,0)
	ICEV-CNG	Conventional vehicle with CNG engine	(1,0,0,1,0,0,0)
BEV	BEV-1	Battery electric vehicle with fixed gear ratio transmission	(0,1,0,0,1,0,1)
	BEV-2	Battery electric vehicle with two-speed transmission	(0,1,0,0,1,0,1)
FCEV	FCHEV	Fuel cell hybrid electric vehicle	(0,1,1,0,1,0,1)
	FCPHEV	Fuel cell plug-in hybrid electric vehicle	(0,1,1,0,1,0,1)
PHEV	PHEV-E10	Plug-in hybrid (P2 configuration) with petrol engine	(1,1,0,0,1,1,1)
	PHEV-CNG	Plug-in hybrid (P2-configuration) with CNG engine	(1,1,0,0,1,1,1)

The vehicle model used is a backward-facing implementation of the longitudinal dynamics. Lateral and vertical vehicle dynamics are assumed to have an insignificant effect on the consumption. Also, no driver model is hence required for following the speed defined in the driving cycle. In a driving resistances equation, the tractive demand at the wheels is calculated as a function of vehicle speed, longitudinal acceleration, road-slope and the assumed vehicle parameters, summarized in Table 3. The vehicle masses, shown for each parametrization in Section 5, is calculated from the base mass of 1150 kg and the parametrization dependent mass of the powertrains.

Table 3: Vehicle parameters for the calculation of traction forces in the driving resistances equation.

Frontal area	Air drag coeff.	Roll res. coeff.	Base mass	Powertrain mass
2,2 m²	0.3	0.008	1150 kg	$f(d)$

As mentioned in Section 2, an efficiency-oriented operating strategy, the Equivalent Consumption Minimization Strategy (ECMS) [12], is applied which decides on gear shifting and the distribution of the tractive demand on ICE and EM, represented by the gear mode gm and the torque split ts. The idea of the ECMS is to define a cost function J comprising an equivalent fuel mass flow of chemical and electric energy that is weighted by the balancing cost factor s. The cost function is minimized in every time step t_i, yielding a locally optimal gear mode gm^* and torque split ts^* in every time step of the simulation.

$$J(gm, ts, t_i) = b_e(gm, ts, t_i) T_{ICE}(gm, ts, t_i) n_{ICE}(gm, t_i) \\ + s \frac{1}{LHV} \frac{1}{\eta_{EM}(gm, ts, t_i) \eta_{batt}} T_{EM}(gm, ts, t_i) n_{EM}(gm, t_i) \quad (2)$$

$$ts^*(t_i), gm^*(t_i) = \arg \min_{ts,gm} J(gm, ts, t_i) \quad (3)$$

Here, b_e denotes the brake specific fuel consumption, T the torque, n the rotational speed, LHV the lower heating value and η the efficiency. With this operating strategy, hybrid operating modes like load point shifting can be chosen if they are identified to be optimal in the current operating point. The energy management of the operating strategy depends on the balancing cost factor s. For vehicles with plug-in functionality, the value of s is determined in a separate iteration loop assuring that the battery is fully depleted at the end of the trip distance[1]. Hybrid vehicles without plug-in functionality, on the other hand, are operated in charge-sustaining

---

[1] If the trip-distance does not exceed the purely electric range of the vehicle, the battery is not depleted.

mode. The exemplary operating behavior of a PHEV in P2-configuration, that results from the described operating strategy, is shown in Fig. 11.

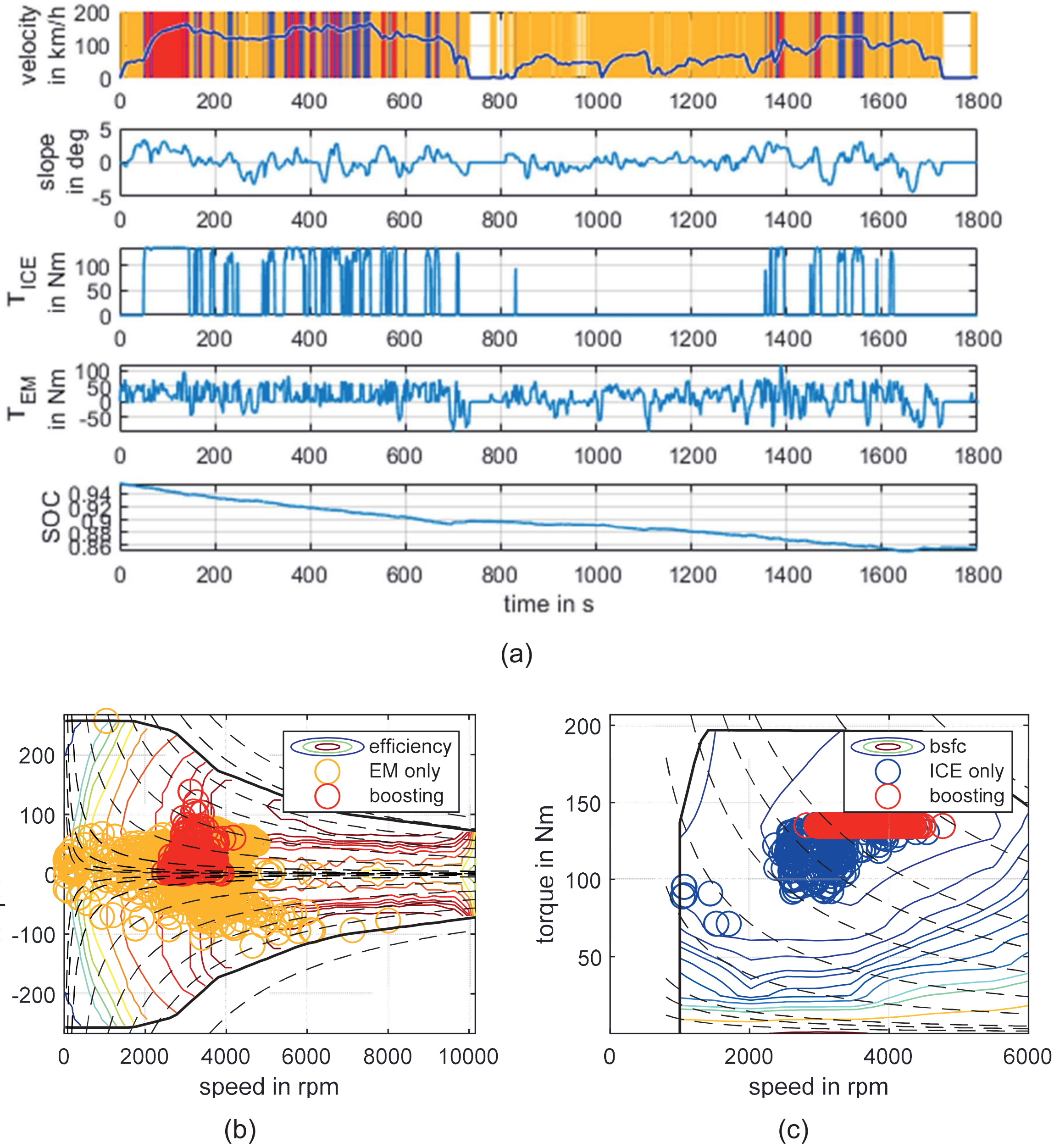

Fig. 11: Exemplary simulation results of the vehicle model for a PHEV-E10 parametrization. SubFig. a) shows the driving cycle, the road-slope and the time-dependent motor torques and state of charge of the battery. The colors indicate operating modes like purely electric driving, combustion engine driving or hybrid modes like boosting for the highest traction power demands. SubFig. b) shows the corresponding operating points of the EM. SubFig. c) shows the operating points of the ICE in the map of brake specific fuel consumption (bsfc).

Concerning the individual powertrain components, we use efficiency maps for the ICE and the EM as functions of torque T and rotational speed n. To differentiate between powertrain parametrizations based on the design parameter set d, multiple scaling approaches are applied to the components. For the EM, a reference efficiency map η_{ref} is defined and a torque-based scaling approach, as in [13], is used to scale the efficiency map as a function of the peak power of the EM $P_{\mathrm{EM,max}}$.

$$\eta_{\mathrm{EM}}(T_{\mathrm{EM}}, n_{\mathrm{EM}}) = \eta_{\mathrm{ref}}(T_{\mathrm{EM}} \frac{P_{\mathrm{ref,max}}}{P_{\mathrm{EM,max}}}, n_{\mathrm{EM}})$$

The efficiency of the FC in our model depends on the momentary power of the FC. The power-dependent efficiency characteristics of a reference FC η_{ref} are scaled to other FC with different peak powers $P_{\mathrm{FC,max}}$ for the simulation of different powertrain parametrizations.

$$\eta_{\mathrm{FC}}(\mathrm{P_{FC}}) = \eta_{\mathrm{ref}}\left(P_{\mathrm{FC}} \frac{P_{\mathrm{FC,ref,max}}}{P_{\mathrm{FC,max}}}\right)$$

Since similar scaling approaches applied to a reference internal combustion engine are assumed to induce larger uncertainties, the ICE is not scaled, but a database of various ICE with different rated powers and efficiency maps is built up. During optimization of a powertrain concept, one of the engines can be selected and its respective power and efficiency characteristics are considered in the vehicle model. The efficiency of the transmission is dependent on the momentary output power and on the powertrain concept, the battery is assumed to have a constant efficiency.

Alongside the efficiency characteristics of the powertrain components, the emissions of the components during production and End-of-Life phases have a considerable effect on the overall GHG emissions. The GHG emissions G_j of component j are therefore calculated based on the constant emission coefficient c_j and the mass of the component m_j, which is a function of the parameter set d.

$$G_j(\boldsymbol{d}) = c_j m_j(\boldsymbol{d})$$

For example, the mass of the EM is made dependent on its peak power $P_{\mathrm{EM,max}}$ and the mass of the battery is dependent on its capacity C_{batt}. Various nonlinear regression curves are derived based on data of existing components to model these characteristics. In Table 4, a summary of the most relevant parameters of the investigated scenario is given, which are relevant to evaluate the GHG emissions and the TED for the different powertrain concepts. The parameters are meant to describe the scenario of Germany in the reference year 2030 and are applied for all results, presented in Section V.

Table 4: Scenario parameters for the estimation of the GHG emissions and the TED.

Description	Value
Fuel supply E10 (GHG)	0,71 kgCO2-eq/kg [2]
Fuel supply CNG (GHG)	0,77 kgCO2-eq/kg [3]
Fuel supply H2 (GHG)	9,83 kgCO2-eq/kg [4]
Power-to-X synthesis efficiency petrol	44,6 %
Power-to-X synthesis efficiency CNG	62 % [5]
Power-to-X synthesis efficiency H2	65,5 % [6]
Production of battery (GHG)	10,17 kgCO2-eq/kg [7]
Production of battery (TED)	Electricity: 9 kWh/kg & Heat: 5,55 kWh/kg [8]
Production of fuel cell (GHG)	17 kgCO2-eq/kW [9]
Production of H2-tank (GHG)	340 kgCO2-eq/kgH2 [10]
Energy density of the Battery	126-170 Wh/kg [11]
Depth of discharge for the Battery	90-95 % dependent on battery size [12]
Specific emissions in the electricity supply	400 gCO2/kWh [13]
Total vehicle mileage	250 000 km [14]

5 Ecological Potential of Different Powertrain Concepts

Within this section, we present the results of the comparative evaluation of the eco-impact of different powertrain concepts in terms of the GHG emissions and the TED. For the first naturalistic driving profile, the pool-vehicle profile, a detailed discussion of the results is given. In

[2] Based on [14].

[3] Based on [14].

[4] Based on [4] with an assumption of 20% H2 via Power-to-X with renewable energies.

[5] Based on [15].

[6] Based on [15, 16].

[7] Based on [4].

[8] Based on [5].

[9] Based on [4].

[10] Based on [4].

[11] Scaling with battery size. Lower limit from [17].

[12] Further improvements for 2030 from study of [5].

[13] Chosen value between [18] and [3].

[14] Annual mileage of diesel vehicles within Germany [19] combined with the mean lifetime of passenger vehicles in Germany [20].

case of the second driving profile, the overall results and differences from the first profile are presented and discussed.

All results were obtained using the presented boundary conditions for the reference year of 2030. As described in Section III, a minimum range of 380 km is imposed to all vehicles. Smaller minimum ranges would lead to different results, as it was studied in previous publications [2]. Especially for BEV class vehicles, the minimum range requirement is a main influencing parameter. For this reason, we additionally investigate the sensitivity of different range requirements for the BEV-2 on the pool-vehicle profile. A comparison to the results from the WLTP is presented in an additional section at the end.

Pool-vehicle profile

The optimized powertrain parametrizations of the different concepts, identified by the optimization framework, are summarized in Table 5. For the concepts with a single energy source (ICEV, BEV, FCHEV), the optimizations towards GHG emissions and TED lead to identical optimal parametrizations. For the plug-in hybrid concepts (FCPHEV & PHEVs) however, the optimal parametrizations differ.

Table 5: Parametrizations of the powertrain concepts, identified by the optimization framework, for the pool-vehicle profile.

concept	objective function	power ICE in kW	power EM in kW	power FC in kW	Battery capacity in kWh	total mass in kg	Max. torque req. in Nm	transmission ratios
ICEV-E10	GHG & TED	140	0	0	0	1278	1911	[7.1 5 3.6 2.7 2.1 1.6 1.3]
ICEV-CNG	GHG & TED	140	0	0	0	1278	1911	[7.1 5 3.6 2.7 2.1 1.6 1.3]
BEV-1	GHG & TED	0	168	0	91,7	1763	2636	4.8
BEV-2	GHG & TED	0	157	0	90,8	1764	2637	[6.1 3.1]
FCHEV	GHG & TED	0	134	91	10	1464	2189	[5.4 2.8]
FCPHEV	GHG	0	140	28	35,6	1576	2357	[6.9 3.1]
PHEV-E10	GHG	96	80	0	35,7	1604	2398	i_{ICE}:[13.5 8.8 5.9 4.2 3.1 2.4 1.9] i_{EM}:1.08*i_{ICE}
PHEV-CNG	GHG	96	78	0	35,6	1598	2389	i_{ICE}:[13.5 9.4 6.7 4.9 3.7 2.9 2.4] i_{EM}:0.88*i_{ICE}
FCPHEV	TED	0	152	21	56,8	1681	2513	[6.4 3.2]
PHEV-E10	TED	71	165	0	85,1	1873	2801	i_{ICE}:[21.4 13.4 8.8 6.0 4.2 3.1 2.4] i_{EM}:0.48*i_{ICE}
PHEV-CNG	TED	96	154	0	59,6	1758	2628	i_{ICE}:[14.8 10.4 7.4 5.4 4.1 3.1 2.4] i_{EM}:0.58*i_{ICE}

Regarding the class of BEV concepts, the BEV-2 normally allows for a significant reduction of the required traction power [2]. This is due to the shiftable transmission, so the launch torque can be achieved with the first transmission speed and the maximum vehicle speed with the second transmission speed. For the BEV-1 on the other hand, the maximum vehicle speed and the launch torque must be achieved with the same transmission ratio. Therefore, to achieve the launch torque for a given transmission ratio, the EM power has to be raised. However, the downsizing potential here is rather small since the pool-vehicle profile is quite dynamic and requires a very high power output irrespective of the design constraints, leading to EM-powers of 168 kW and 157 kW for the BEV-1 and BEV-2. Due to the slightly downsized EM and the shiftable transmission, the BEV-2 allows for a reduction of electric consumption in the usage phase (see Fig. 12), which additionally enables to reduce the installed battery capacity. On the other hand, the two-speed transmission is heavier than the fixed-speed transmission of the BEV-1, hence the total vehicle masses of both vehicles are almost identical.

The vehicles of the FCEV class were equipped with a two-speed electric drive since this is beneficial for the GHG emissions and the TED, as previously discussed for the BEV vehicles. For the FCEV class, the plug-in variant requires a larger EM power due to a higher total vehicle mass mainly caused by a larger battery capacity. The power of the fuel cell is significantly lower for the plug-in variant, since enough energy and power support can be provided by the larger battery capacity for longer high traction power phases. The battery capacity of 10 kWh for the FCHEV, which is operated in charge sustaining mode, is necessary to provide enough combined electric power of fuel cell and battery to boost in high traction demands and for recuperation. For the FCPHEV, a battery capacity of ~35 kWh for the GHG optimization and ~57 kWh for the TED optimization are calculated. Both allow for a very high electric range to limit the use of H2. However, to minimize the TED, a higher battery capacity is even more beneficial than to minimize the GHG emissions.

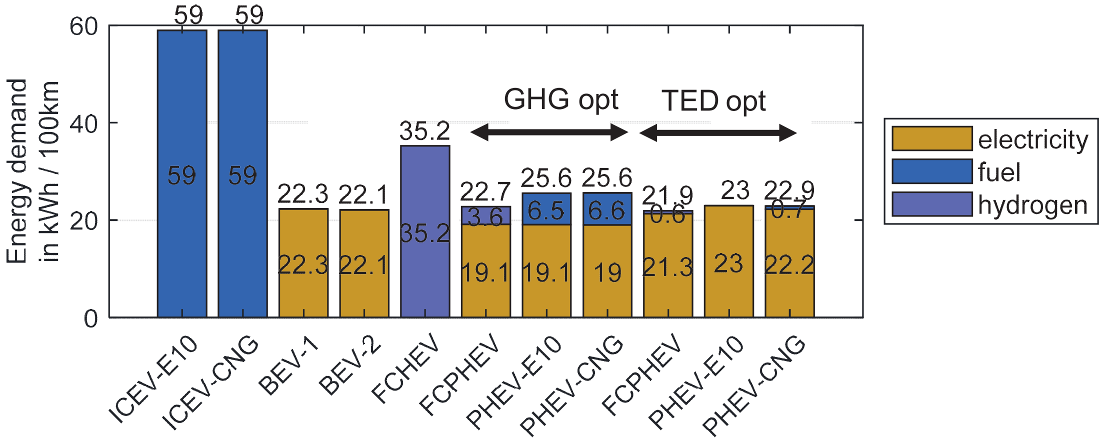

Fig. 12: Energy demands of the different powertrain concepts in the usage phase (1 liter petrol-E10 corresponds to 8.95 kWh, 1 kg H2 corresponds to 33.42 kWh, 1 kg CNG corresponds to 12.83 kWh).

The parametrization of the two PHEV concepts optimized towards the GHG emissions are pretty similar. Both have EM powers of around 80 kW and battery capacities of around 35 kWh, which allow to achieve a high electric driving percentage up to the driving cycle of the third distance cluster with a distance of 155 km (see Section III for details). For higher distances, it is preferable to use the combustion engine instead of further increasing the battery capacity in order to minimize the GHG emissions. For the TED optimization of the PHEV concepts on the other side, higher battery capacities are chosen to limit the energy demand in the Power-to-X fuel synthesis resulting in a parametrization that can drive almost purely electric for the E10-variant. The PHEV-E10, optimized towards the TED, is the heaviest vehicle since it is equipped with a high battery capacity (~85 kWh) and the combined components of the hybrid powertrain. The synthesis of CNG via Power-to-X is less energy intensive than the synthesis of petrol, which is why the battery capacity is set to ~60 kWh for the PHEV-CNG, relying on a minor use of CNG on the highest distance tracks.

The results concerning the GHG emissions of the different concepts are summarized in Fig. 13. The different parametrizations of the same concept resulting from the two objective functions have a noticeable effect on the GHG emissions. As a first general conclusion, it can be seen that the electrification of the powertrains is essential, since the conventional powertrain concepts lead to the highest GHG emissions. Concerning the BEV class concepts, the BEV-2 shows slightly better results than the BEV-1. In the FCEV class, a plug-in option is very beneficial, since it allows to make use of the efficient electric path from the charging station trough the battery to the EM. Using H2, on the other hand, is less efficient and also causes high GHG emissions in the fuel supply as shown in Table 4. The FCPHEV concept achieves the lowest GHG emissions for this scenario.

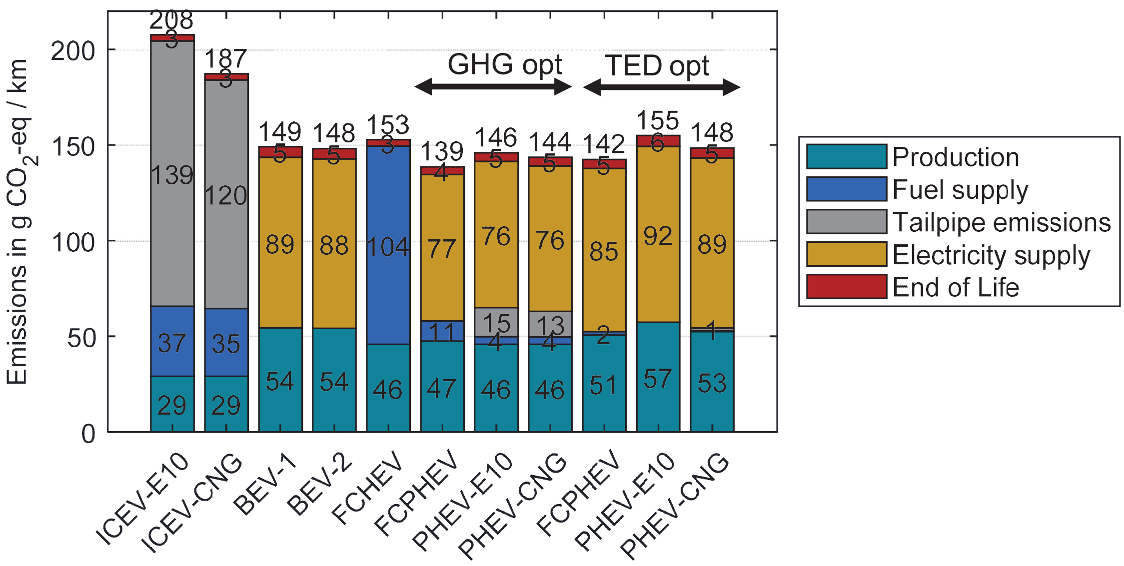

Fig. 13: GHG emissions of the powertrain concepts identified by the optimization framework for the pool-vehicle profile with GHG emissions and TED as objective functions. For the ICEV and BEV class concepts and the FCHEV, the powertrain parametrizations are identical for both objective functions and are therefore displayed with one bar respectively.

The PHEV concepts which were optimized towards the GHG emissions show, by a small margin, worse results concerning the GHG emissions than the FCPHEV. The reduced battery capacity compared to the BEV concepts still allows for a high percentage of electric driving, but reduces the emissions in the production phase significantly. It is beneficial for the PHEV to drive long distances with the help of the combustion engine, which results in 15 and 13 g CO2/km of tailpipe emissions for E10 and CNG, respectively. Due to the lower emissions in the supply of CNG compared to petrol, the PHEV-CNG achieves lower emissions than the PHEV-E10.

If the use of Power-to-X with renewable energies would be partly assumed for CNG in the year 2030, as it was done for H2 within this study, the GHG emissions of the PHEV-CNG would further improve. Another fundamental difference between the PHEV and the FCPHEV is the use of the ICE and the EM in parallel mode for traction, which is not possible for the fuel cell. Therefore, the parametrizations of the PHEV offer greater acceleration reserves and could be especially suited for premium class vehicles.

The resulting TED of the optimized powertrain parametrizations is shown in Fig. 14. Since the fuel supply via power-to-X is very energy intensive, the conventional concepts lead by far to the highest TED. The FCHEV without plug-in option suffers from the same problem and leads to a relatively high TED. All concepts with a direct plug-in option achieve significantly better

TED values since they profit from the high efficiency of the electric path. The BEV concepts achieve values very close to their mean electric consumption. The difference between the TED and the mean electric consumption results from battery production. For the plug-in hybrid concepts (FCPHEV and PHEV), the TED values differ dependent on the objective function of the optimization. The plug-in hybrid concepts, optimized to reduce GHG emissions, lead to higher TED values, since they still partly rely on the use of H2, petrol or CNG. To achieve a minimum TED, it is better to increase the battery capacity to further limit the necessary amount of fuel synthesis via Power-to-X.

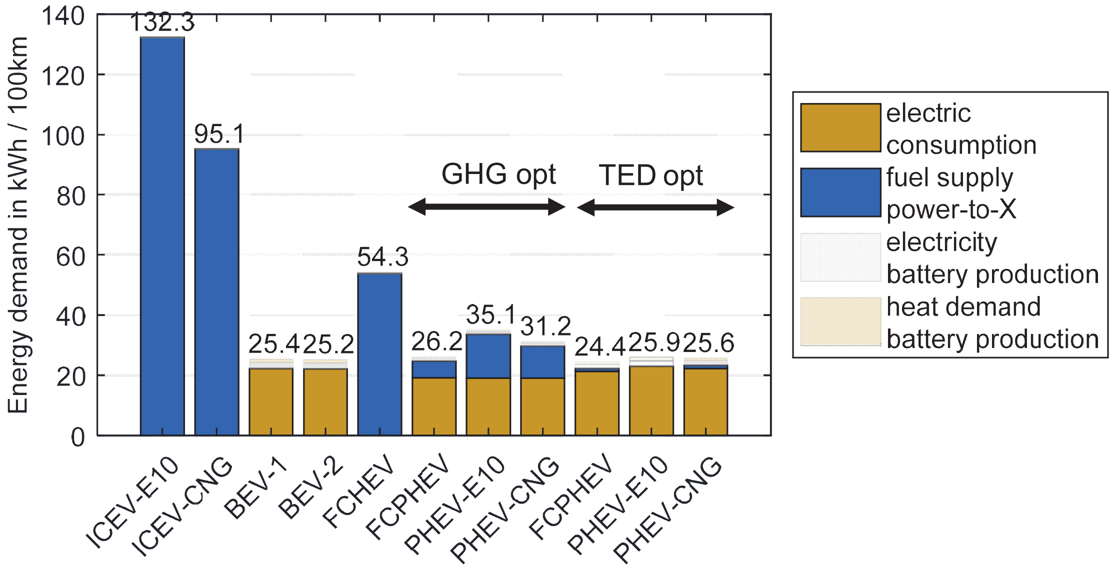

Fig. 14: TED of the powertrain concepts identified by the optimization framework for the pool-vehicle profile with GHG emissions and TED as objective functions.

The FCPHEV shows a very good performance for both optimization criteria. Firstly, the synthesis efficiency for H2 is higher than for petrol or methane. Therefore, even the GHG-optimized FCPHEV achieves a relatively good TED of 26.2 kWh/100 km. Secondly, the mean efficiency of the FC is higher compared to the ICE. Thirdly, the vehicle weight of the FCPHEV is slightly smaller compared to the PHEV concepts. The combined weight of the fuel cell and the H2-tank in our model are less than the weight of the combustion engine, the more complex transmission and the exhaust gas treatment.

As mentioned before, the GHG emissions of the BEV are highly dependent on the minimum range requirement in contrast to all other powertrain concepts which would only need a larger fuel tank.

The GHG emissions of the BEV-2 based on the pool-vehicle profile for different range requirements are summarized in Table 6. When compared to the nearly constant values of 144 and

139 g CO2/km for the PHEV-CNG and FCPHEV, respectively, the BEV class proves to be suitable only for smaller range requirements.

Table 6: GHG emissions of the BEV-2 concept for the pool-vehicle profile with different maximum range requirements. For each range, a separate optimization of the powertrain parameters has been performed. The base scenario corresponds to the longest track of the profile with a 10% buffer.

BEV-2	Values			
Range in km	250	300	380	450
GHG in gCO2/km	142	145	148	155
Battery capacity in kWh	68	81.9	90.8	109.8
El. Consumption in kWh/100km	21.6	21.9	22.1	22.6
Vehicle weight in kg	1665	1726	1764	1879

Employee profile

The parametrization of the optimized powertrain concepts for the employee profile are summarized in Table 7. Again, the parametrizations of the concepts with a single energy source are identical for both objective functions. For the plug-in hybrid concepts, on the other hand, the resulting optimal parametrizations deviate for both objective functions.

Due to the more efficiency-oriented and calm driving of this profile compared to the pool-vehicle, a significant reduction in installed power is possible for all concepts. Further, this leads to a reduction of the energy demands during operation, as shown in Fig. 15, and a smaller battery capacity for the BEV concepts, compared to the pool-vehicle profile.

Table 7: Parametrizations of the powertrain concepts identified by the optimization framework for the employee profile.

concept	objective function	power ICE in kW	power EM in kW	power FC in kW	Battery capacity in kWh	total mass in kg	Max. torque req. in Nm	transmission ratios
ICEV-E10	GHG & TED	96	0	0	0	1261	1885	[11.4 7.6 5.2 3.6 2.6 1.9 1.4]
ICEV-CNG	GHG & TED	96	0	0	0	1261	1885	[11.4 7.4 5 3.4 2.4 1.8 1.3]
BEV-1	GHG & TED	0	124	0	63,1	1630	2437	6.4
BEV-2	GHG & TED	0	118	0	62,4	1633	2442	[8.5 4.2]
FCHEV	GHG & TED	0	100	40	6,2	1380	2062	[7.3 3.7]
FCPHEV	GHG	0	102	41	9,4	1407	2103	[8.4 4.3]
PHEV-E10	GHG	71	50	0	27,6	1528	2284	i_{ICE}:[17.5 10.7 6.9 4.6 3.3 2.4 1.9] i_{EM}:1.14*i_{ICE}
PHEV-CNG	GHG	96	43	0	10,3	1398	2090	i_{ICE}:[11.8 7.1 4.6 3.2 2.3 1.9 1.6] i_{EM}:1.37*i_{ICE}
FCPHEV	TED	0	113	42	27,4	1538	2300	[8.9 3.9]
PHEV-E10	TED	71	63	0	34,9	1579	2360	i_{ICE}:[18.1 11.7 7.7 5.2 3.6 2.5 1.8] i_{EM}:0.82*i_{ICE}
PHEV-CNG	TED	71	64	0	34,8	1579	2360	i_{ICE}:[18.1 11.9 7.9 5.4 3.7 2.6 1.9] i_{EM}:0.81*i_{ICE}

In the case of the plug-in hybrid concepts, the battery capacity is also reduced in comparison to the previous profile. The reason for this lies in the distance distribution of driven kilometers shown in Fig. 7. As can be seen, a higher percentage of the kilometers are driven on trips bellow a distance of 100 km, compared to the pool-vehicle profile. Therefore, a smaller battery capacity is sufficient to achieve a high electric driving percentage for the hybrid vehicles, which is beneficial for the GHG emissions and the TED.

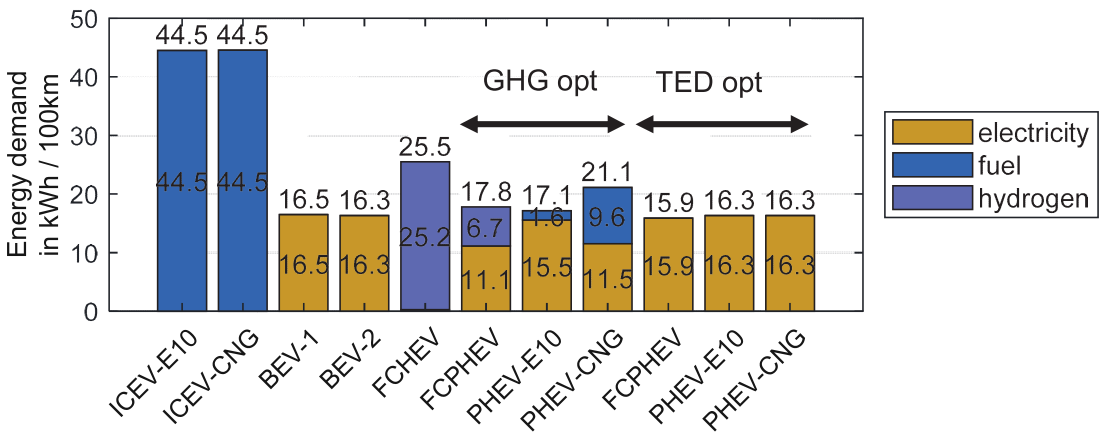

Fig. 15: Energy demands of the different powertrain concepts in the usage phase for the employee profile (1 liter petrol-E10 corresponds to 8.95 kWh, 1 kg H2 corresponds to 33.42 kWh, 1 kg CNG corresponds to 12.83 kWh).

The resulting minimal GHG emissions are presented in Fig. 16. As mentioned before, the more efficiency-oriented driving results in lower GHG values for all concepts compared to the pool-vehicle profile. However, the relative ranking of the concepts stays similar and previously drawn conclusions are confirmed.

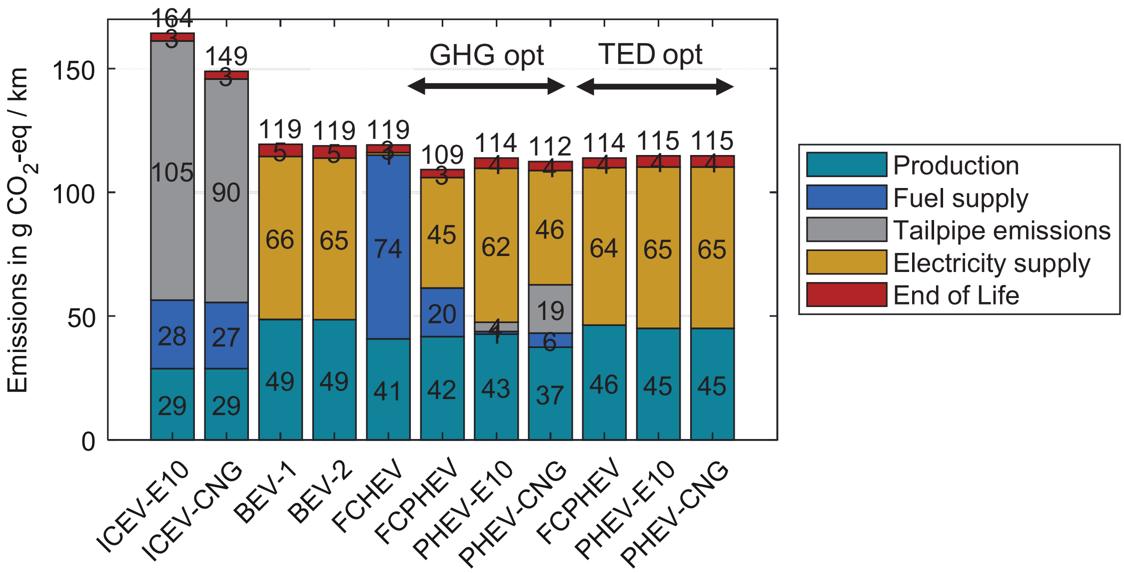

Fig. 16: GHG emissions of the powertrain concepts identified by the optimization framework for the employee profile with GHG emissions and TED as objective functions.

An electrification of the powertrain concepts is essential. For the FCEV class, a plug-in option is beneficial to reduce the GHG emissions and the TED. The FCPHEV and the PHEV-CNG can achieve the best GHG emission values, when they are parametrized to specifically minimize the GHG. For the employee profile, the plug-in hybrid concepts show a larger percentage benefit over the BEV concepts, which is due to the higher occurrence of shorter trips in this profile, that can be driven mostly electrically with a smaller battery by the plug-in hybrid concepts. For the PHEV-CNG concept, it is beneficial to rely on a significant use of the combustion engine in case of the GHG optimization instead of increasing the battery capacity. For the petrol-E10 counterpart, the fuel consumption is limited by an increased battery capacity and more electric driving.

Regarding the TED, the results are shown in Fig. 17. According to the results for the GHG emissions, the minimum achievable TED values are also reduced, compared to the pool-vehicle profile, due to the calmer driving profile. The plug-in hybrid concepts, optimized towards the TED, allow for a smaller TED than the BEV concepts. Their battery capacity of around 30 kWh is sufficient to complete the representative driving cycle of the highest distance cluster with 210 km almost purely electrically. At the same time, the reduced power of the EM allows for the operation of the EM with higher efficiencies in electric driving situations, due to higher specific power utilization, compared to the BEV concepts. Additionally, the higher number of gear modes of the transmission can be used during purely electric driving, further increasing the efficiency.

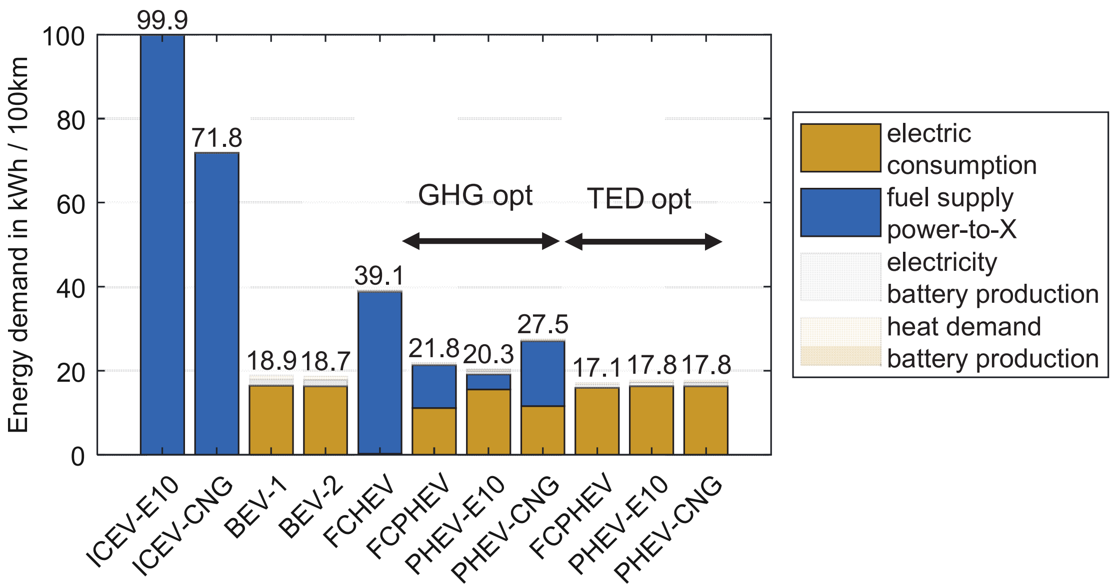

Fig. 17: TED of the powertrain concepts identified by the optimization framework for the employee profile with GHG emissions and TED as objective functions.

Worldwide harmonized Light vehicles Test Procedure

As described at the end of Section III, we evaluate the previously presented powertrain parametrizations on the WLTP and compare the results to the determined GHG emissions. The relevant values are summarized in Table 8. The vehicles from the optimization towards the GHG emissions for the employee profile are considered for the comparison, which means that all values result from the vehicle simulation with the parametrizations presented for the employee profile. Additionally, the CO2 emissions resulting from the WLTP evaluation, which only consider the tailpipe emissions, the previously determined total GHG emissions and the TED are compared.

Table 8: Evaluation of the CO2 emissions of the vehicle parametrizations from the employee profile according to the WLTP. The results from the consideration of the total GHG emissions and the TED are denoted for the comparison from the GHG-optimal powertrains.

	units	ICEV-E10	ICEV-CNG	BEV-1	BEV-2	FCHEV	FCPHEV	PHEV-E10	PHEV-CNG
WLTP									
utility factor	~	0	0	1	1	0	0,92	0,97	0,90
petrol	l/100km	4,7						0,1	
CNG	kg/100km		3,2						0,6
H2	kg/100km					0,6	0,3		
elecricity	kWh/100km			12,9	12,8		6,8	12,1	8,6
tailpipe emissions	gCO2/km	96	83	0	0	0	0	2	17
Ecological impact on employee profile									
GHG	gCO2/km	164	149	119	119	119	109	114	112
TED	kWh/100km	100	72	19	19	39	22	20	28

From the comparison, it is clear that the evaluation according to the WLTP is not suited to measure the eco-impact considering the complete GHG emissions. This is plausible since the WLTP does only consider direct tailpipe emissions. The GHG emissions of all powertrain concepts are underestimated. Especially the emissions of 0 gCO2/km for BEV and FCEV vehicles are misleading. Furthermore, regarding the eco-impact according to the TED, the WLTP leads to wrong conclusions. For example, the benefit of the plug-in option for FCEV concepts shown in this work is not getting transparent. Also, the previously determined low GHG emissions and TED values of the PHEV-CNG cannot be concluded by the evaluation according to the WLTP. Despite these issues, the evaluation according to the WLTP is the established process, used by policy makers to induce changes to the vehicle market. For example, the average fleet emissions of manufacturers, limited to 95 gCO2/km for 2020 by the European Commission, are determined using the WLTP. The authors believe that the current homologation process leads to distorted incentives in the reduction of the ecological impact and that the introduction of a more suited evaluation procedure would improve the effectiveness in achieving the goal of a more ecological mobility.

6 Conclusions

In this contribution, we present a data-driven optimization framework for the comparative evaluation of the eco-impact of different powertrain concepts. Naturalistic driving profiles, containing the occurrence frequency of operating states in the speed, acceleration and road-slope dimension are the basis for the evaluation. Representative and multidimensional driving cycles are generated to depict the driving profiles in a compressed manner within the optimization framework. The representative cycles allow for an efficient search of the optimal powertrain parametrizations in the optimization. Since the ecological potential of all powertrain concepts is identified with this framework, an equal and unbiased evaluation basis is generated to compare different powertrain concepts. We investigate the GHG emissions and the Total Energy Demand (TED) of vehicles with long-range capability for the reference year of 2030 in Germany. In our study, most of the currently discussed powertrain classes (BEV, FCEV, PHEV) are included to provide a comprehensive comparison of the ecological potential of the presented concepts on a uniform evaluation basis.

Important conclusions can be drawn from our study of two exemplary naturalistic driving profiles:

The driving profile itself has a significant impact on the GHG emissions and the TED. For example, the calm and efficiency-oriented driving style of the employee profile leads to a reduction of 19,6-22,2 % of the GHG emissions, for the concepts that were optimized towards the GHG emissions, compared to the pool-vehicle profile. This shows that the use of real-driving profiles from the relevant application should be used to ensure that the real ecological impact of the vehicles is estimated.

The results of both driving profiles show that the electrification of powertrain concepts is essential to reduce the GHG emissions and the TED. Conventional vehicles have the lowest potential of the studied powertrain concepts to reduce the eco-impact by 2030.

The class of BEV leads to improvements compared to the ICEV class. Within the BEV class, a shiftable transmission, enables to reduce the power of the EM, the electric consumption, the battery size and therefore both the GHG emissions and the TED.

For the plug-in hybrid concepts (FCPHEV and PHEV), the parametrization of the concepts differs dependent on the objective function of the optimization. To minimize the GHG emissions, a smaller battery capacity compared to the BEV concepts already allows for a high electric driving percentage. The use of fuels to manage high distance tracks is preferred instead of further increasing the battery capacity, which would lead to higher vehicle weights and relevant emissions in the production phase. To minimize the TED on the other hand, higher battery capacities are advantageous to limit the use of fuels, which have to be synthesized via Power-to-X with a relatively low efficiency.

The suitability of plug-in hybrid concepts for a reduction of the eco-impact is highly dependent on the distance distribution of tracks in the driving profile. For profiles with a significant share of shorter distance trips, the battery capacities of the plug-in hybrid concepts can be relatively small without diminishing the electric driving percentage. Therefore, on such profiles the benefit of the plug-in hybrid concepts over the BEV increases. Conversely, if most tracks are of a high distance, the battery of the plug-in hybrid concepts and BEV will be dimensioned similarly and the benefits become smaller. However, in our model, we assume a fully charged battery before each trip for the plug-in hybrid concepts. Therefore, this ecological potential of the hybrid vehicles can only be achieved with a suited user behaviour and regular charging. Unregular charging, on the other hand, would increase the GHG emissions and the TED of the plug-in hybrid concepts significantly.

In the class of FCEV, a plug-in option is identified to be very beneficial for the eco-impact of these concepts. The plug-in option enables to make use of the higher efficiency electric path and enables to reduce the required H2-tank size.

The PHEV concepts achieve reduced GHG emissions compared to the BEV concepts for both investigated profiles. The high electric driving percentage with a reduced battery capacity and vehicle weight is one of the main reasons for this. At the same time, the power of the EM of the GHG-optimized PHEV is smaller compared to BEV vehicles, since the ICE allows to fulfil the highest traction demands by boosting. In the less demanding driving situations, which occur much more frequently, the lower EM power allows for a higher specific power utilization of the EM and therefore the operation in generally more efficient operating points.

Within our contribution, monetary costs have not been considered. Certainly, the ecological return on monetary invest is relevant for the comprehensive comparison of different powertrain concepts and should be further studied. Additional expenses regarding necessary infrastructure could also be included in the investigation. Certainly, the PHEV concepts demand the least adaptions of currently available infrastructure despite the conventional ICEV concepts.

Generally, the three concepts BEV-2, FCPHEV and PHEV-CNG were identified to have the best ecological potential. The plug-in hybrid concepts are especially suited when the distance-distribution is characterized by a high percentage of driven kilometers in the lower distance range while maintaining the requirement of long-range capability.

As additional investigation, we compared the GHG emissions resulting from the evaluation according to the WLTP to the presented comprehensive evaluation. We showed that the obvious discrepancies in the assessment between our holistic approach and the WLTP lead to non-optimal incentives in the design of powertrain concepts. In order to support the development of real-world efficient eco-friendly vehicles, the certification process should be further adapted.

Literature

[1] IPCC, “Climate change 2014 - Synthesis report: Contribution of Working Groups I, II and III to the Fifth Assessment Report of the Intergovernmental Panel on Climate Change [Core Writing Team, R.K. Pachauri and L.A. Meyer (eds.)]. IPCC, Geneva, Switzerland, 151 pp.,” 2014.

[2] A. Esser, J.-E. Schleiffer, T. Eichenlaub, and S. Rinderknecht, “Development of an Optimization Framework for the Comparative Evaluation of the Ecoimpact of Powertrain Concepts,” In: 19. Internationaler VDI-Kongress "Dritev - Getriebe in Fahrzeugen", Bonn, 10.-11. Juli 2019, In: VDI-Berichte, 2354, ISBN 978-3-18-092354-3, 2019.

[3] M. Wietschel, M. Kühnbach, and D. Rüdiger, “Die aktuelle Treibhausgas- emissionsbilanz von Elektrofahrzeugen in Deutschland: Working Paper Sustainability and Innovation No. S 02/2019,” 2019.

[4] F. ISE, “Treibhausgas-Emissionen für Batterie- und Brennstoffzellenfahrzeuge mit Reichweiten über 300 km,” 2019.

[5] J. F. Peters and M. Weil, “Providing a common base for life cycle assessments of Li-Ion batteries,” *Journal of Cleaner Production*, vol. 171, pp. 704–713, 2018, doi: 10.1016/j.jclepro.2017.10.016.

[6] A. Esser, M. Zeller, S. Foulard, and S. Rinderknecht, “Stochastic Synthesis of Representative and Multidimensional Driving Cycles,” *SAE Int. J. Alt. Power.*, vol. 7, no. 3, pp. 263–272, 2018, doi: 10.4271/2018-01-0095.

[7] MathWorks, *Genetic Algorithm.* [Online]. Available: https://www.mathworks.com/help/gads/ga.html (accessed: Sep. 9 2019).

[8] J. Lin and D. A. Niemeier, “Regional driving characteristics, regional driving cycles,” *Transportation Research Part D: Transport and Environment*, vol. 8, no. 5, pp. 361–381, 2003, doi: 10.1016/S1361-9209(03)00022-1.

[9] J.-M. Zaccardi and F. Le Berr, “Analysis and choice of representative drive cycles for light duty vehicles – case study for electric vehicles,” *Proceedings of the IMechE*, vol. 227, no. 4, pp. 605–616, 2013, doi: 10.1177/0954407012454964.

[10] T. G. Farr *et al.,* “The Shuttle Radar Topography Mission,” *Reviews of Geophysics*, vol. 45, no. 2, 2007, doi: 10.1029/2005RG000183.

[11] P. Jardin, A. Esser, S. Givone, T. Eichenlaub, J.-E. Schleiffer, and S. Rinderknecht, “The Sensitivity in Consumption of Different Vehicle Drivetrain Concepts Under Varying Operating Conditions: A Simulative Data Driven Approach,” *Vehicles*, vol. 1, no. 1, pp. 69–87, 2019, doi: 10.3390/vehicles1010005.

[12] G. Paganelli, S. Delprat, T. M. Guerra, J. Rimaux, and J. J. Santin, “Equivalent consumption minimization strategy for parallel hybrid powertrains,” in *IEEE 55th Vehicular Technology Conference*, Birmingham, AL, USA, 2002, pp. 2076–2081.

[13] A. Balazs, *Optimierte Auslegung von Hybridantriebsträngen unter realen Fahrbedingungen*. Fakultät für Maschinenwesen, RWTH Aachen, Dissertation, 2015.

[14] B. Belmonte, Esser, Weyand, Franke, Schebek, and Rinderknecht, “Identification of the Optimal Passenger Car Vehicle Fleet Transition for Mitigating the Cumulative LifeCycle Greenhouse Gas Emissions until 2050,” *Vehicles*, vol. 2, no. 1, pp. 75–99, 2020, doi: 10.3390/vehicles2010005.

[15] FVV, Ed., “Defossilisierung des Transportsektors,” 2018. [Online]. Available: https://www.fvv-net.de/fileadmin/user_upload/medien/materialien/FVV__Kraftstoffe__Studie_Defossilisierung__R586_final_v.3_2019-06-14__DE.pdf

[16] FVV, Ed., “Energiepfade für den Straßenverkehr der Zukunft: Optionen für eine klimaneutrale Mobilität im Jahr 2050,” 2018. [Online]. Available: https://www.fvv-net.de/fileadmin/user_upload/medien/materialien/FVV__Kraftstoffe__Studie_Energiepfade__final_v.3_2018-10-01__DE.pdf

[17] A. Thielmann, A. Sauer, R. Isenmann, and M. Wietschel, *Technology roadmap energy storage for electric mobility 2030.* [Online]. Available: https://www.isi.fraunhofer.de/content/dam/isi/dokumente/cct/lib/TRM-ESEM-2030_en.pdf (accessed: Sep. 19 2018).

[18] H. Helms, Julius Jöhrens, Jan Hanusch, Ulrich Höpfner, Udo Lambrecht, and Martin Pehnt, *UMBRELA: Wissenschaftlicher Grundlagenbericht gefördert durch das Bundesministerium für Umwelt, Naturschutz und Reaktorsicherheit (BMU)* (accessed: May 16 2018).

[19] statista, *Fahrleistung der Pkw in Deutschland im Jahr 2018 (in Kilometern).* [Online]. Available: https://de.statista.com/statistik/daten/studie/246069/umfrage/laufleistung-privater-pkw-in-deutschland/ (accessed: Sep. 25 2019).

[20] Plötz, Gnann, Kühn, and Wietschel, “Markthochlaufszenarien für Elektrofahrzeuge,” 2013.